Journal of Nuclear Materials 385 (2009) 392–399

Contents lists available at ScienceDirect

Journal of Nuclear Materials

journal homepage: www.elsevier.com/locate/jnucmat

Design of a fuel element for a lead-cooled fast reactor

V. Sobolev *, E. Malambu, H. Aït Abderrahim

SCK•CEN, Belgian Nuclear Research Centre, Boeretang 200, B-2400 Mol, Belgium

ARTICLE INFO

PACS:
28.41.–i
28.41.Ak
28.41.Bm
28.50.Ft

ABSTRACT

The options of a lead-cooled fast reactor (LFR) of the fourth generation (GEN-IV) reactor with the electric power of 600 MW are investigated in the ELSY Project. The fuel selection, design and optimization are important steps of the project. Three types of fuel are considered as candidates: highly enriched Pu–U mixed oxide (MOX) fuel for the first core, the MOX containing between 2.5% and 5.0% of the minor actinides (MA) for next core and Pu–U–MA nitride fuel as an advanced option. Reference fuel rods with claddings made of T91 ferrite–martensitic steel and two alternative fuel assembly designs (one uses a closed hexagonal wrapper and the other is an open square variant without wrapper) have been assessed. This study focuses on the core variant with the closed hexagonal fuel assemblies. Based on the neutronic parameters provided by Monte–Carlo modeling with MCNP5 and ALEPH codes, simulations have been carried out to assess the long-term thermal–mechanical behaviour of the hottest fuel rods. A modified version of the fuel performance code FEMAXI-SCK-1, adapted for fast neutron spectrum, new fuels, cladding materials and coolant, was utilized for these calculations. The obtained results show that the fuel rods can withstand more than four effective full power years under the normal operation conditions without pellet–cladding mechanical interaction (PCMI). In a variant with solid fuel pellets, a mild PCMI can appear during the fifth year, however, it remains at an acceptable level up to the end of operation when the peak fuel pellet burnup ~80 MW d kg^{-1} of heavy metal (HM) and the maximum clad damage of about 82 displacements per atom (dpa) are reached. Annular pellets permit to delay PCMI for about 1 year. Based on the results of this simulation, further steps are envisioned for the optimization of the fuel rod design, aiming at achieving the fuel burnup of 100 MW d kg^{-1} of HM.

1. Introduction

In the Generation IV International Forum documents [1] the lead-cooled fast reactor (LFR) is considered as one of three concepts of new generation fast nuclear systems that can be used for both electricity production and transuranium elements (TRU) incineration – a way for closing the nuclear fuel cycle. In order to insure a high efficiency of the LFR operation and requirements of non-proliferation, a long fuel residence time in the core (5 years or more) is sought. Improvement of the utilization of fuel resources and of the nuclear plant economical performances requires reaching a fuel discharge burnup of 80–100 MW d kg^{-1} of heavy metal (HM: U, Pu, etc.). Different LFR systems are considered in different countries: BREST [2] and SVBR [3] in the Russian Federation, PBWFR [4], SLPLFR [5] and CANDLE [6] in Japan, PEACER [7] and BORIS [8] in Korea, SSTAR [9] in the USA and ELSY [10] in the EU. The fuel selection and pre-design, the core design, the fuel behaviour simulation and the fuel design optimization are important steps in these programs. BREST, PBWFR, CANDLE, BORIS and SSTAR reactors are opted for nitride fuel, PEACER for metallic, SVBR and ELSY for oxide or nitride fuels.

The European Lead-cooled SYstem (ELSY) with the electric power of 600 MW is under design studies in the 6th framework program of EURATOM [11]. In the ELSY-600 reactor, three fuel types are considered as candidates, namely: highly enriched Pu–U mixed oxide fuel (MOX), the MOX containing from 2.5 to 5.0 wt% of the minor actinides (MA: Np, Am, Cm) in HM, and nitride fuel as an advanced future option. The highly enriched MOX is the first option with which the first ELSY core will start. Later it will progressively be filled in with the MA containing oxide fuel. In the frameworks of the ELSY Project, reference fuel rods with the cladding made of the ferrite–martensitic steel T91 and two alternative variants of the fuel assembly: one with a hexagonal close wrapper and the other with a square cross-section but without wrapper – are assessed, fulfilling the LFR GEN-IV requirements [11]. The ELSY-600 design variant with the hexagonal MOX fuel assemblies, called here LFR-600, was used as a basis for the simulation and analysis of the long-term behaviour of the hottest MOX fuel rods at the LFR representative conditions.

2. Fuel element and core materials and specifications

In the first core of LFR-600, the highly enriched MOX with 14–20% Pu in HM and density close to 95% of the theoretical density

* Corresponding author. Tel.: +32 14 33 22 67; fax: +32 14 32 15 29.
E-mail address: vsobolev@sckcen.be (V. Sobolev).

0022-3115/$ - see front matter © 2008 Elsevier B.V. All rights reserved.
doi:10.1016/j.jnucmat.2008.12.027

(TD) is selected to use. Concerning the oxygen stoichiometry, the oxygen to metal atomic ratio of O/M = 1.97 is temporarily fixed based on the previous experience with MOX fuels. The typical isotopic vector of the reactor grade Pu, extracted from the spent UO_2 fuel of a typical PWR (initial enrichment 4.5% ^{235}U, burnup 45 MW d kg^{-1}, 15 years of cooling and storage), and the depleted uranium blended with the reprocessed uranium (often used for the industrial production of MOX) were taken for the pre-design calculations (Table 1).

In order to insure high efficiency of the reactor operation along with the requirements of non-proliferation, a long residence time of fuel in the core should be sought. This will mainly be determined by the permitted resistance time of the fuel and cladding materials at the designed basis operational conditions. In the case of LFR, the resistance of the pin cladding to corrosion attack by the liquid lead coolant (Pb) will play a major role. The choice of the cladding material and of the temperature range of the Pb-coolant operation is of utmost importance for both the safety and the economics of the reactor.

A margin to solidification (the Pb melting temperature is 600.6 K) imposes to use the coolant minimum temperature of at least 673 K (400 °C) [11]. The maximum coolant temperature is limited by the strong corrosion of well-known cladding materials in Pb at temperatures higher then 823 K (550 °C). The available experience of using Pb and Pb–Bi eutectic shows that the coolant bulk velocity has to be lower than 2 m s^{-1}, in order to avoid erosion problems during long-term operation in the temperature region of 673–823 K (400–550 °C) [12].

Ferritic–martensitic steels (FMS) are considered among the best candidates for the cladding material of the fast nuclear reactors with heavy liquid metal coolants. At temperatures higher than 673 K (400 °C) they show a lower irradiation induced swelling and creep rates [13], a better resistance to dissolution in the oxygen-free Pb compared to austenitic steels [14,15] and a reasonable irradiation induced embrittlement. A higher oxidation rate of FMS can successfully be managed by the control of oxygen dissolved in Pb-alloy coolant by utilizing the technology firstly developed in Russia [16] and then customized in Europe [17]. The existing laboratory studies on the compatibility of different structural materials with molten Pb and Pb–Bi eutectic show that some steels can resist corrosion attack by the liquid metal for about 25 000 h in a flow with velocity up to 2.0 m s^{-1} and temperature of 833 K (560 °C) under oxygen controlled conditions. The small thickness of the formed oxide layer permits a prognosis that the operation time of these steels might be extended to about 50 000 h [12]. There is, however, no similar experience under in-pile reactor conditions. New developments show that coating of the T91 cladding surface with a FeCrAlY alloy using the GEZA technique allows to form a more stable oxide protective layer that can insure the long-term operation in Pb–Bi flow at temperatures up to 873 K (600 °C) under the optimized oxygen content ($\sim 10^{-6}$ wt%) in the coolant [18]. For these reasons FMS T91 is chosen as the LFR-600 fuel-cladding material. A period of 5 years, as determined by the corrosion limit, is adopted for the fuel element residence time.

Table 1
The isotopic vectors of plutonium and uranium used in calculations.

Plutonium		Uranium	
Isotope	Fraction (wt%)	Isotope	Fraction (wt%)
^{238}Pu	2.332	^{234}U	0.003
^{239}Pu	56.873	^{235}U	0.404
^{240}Pu	26.997	^{236}U	0.010
^{241}Pu	6.105	^{238}U	99.583
^{242}Pu	7.693		

Two more factors can also limit the residence time of the fuel element in the core. These are the foreseen fuel burnup and the cladding damage. The maximum burnup is mainly limited by the cladding resistance to the pressure of the released fission gas and to the fuel-cladding mechanical and chemical interaction. The experience of operation of LMFBR fueled with Pu–U MOX shows that burnup up to 100 MW d kg^{-1} can be reached without problems [19,20]. This value was adopted as the targeted discharge burnup for the hottest fuel assembly of the first LFR-600 core. (Note that this value is about a factor of two less than that targeted in the European fast reactor project [21–23].)

The cladding damage and the fuel burnup are in close correlation. In the preliminary modeling of Pb-alloy cooled fast reactors, a damage of about one atomic displacement per atom (dpa) in the T91 cladding per 1 MW d kg^{-1} of HM burnup in MOX was obtained [24]. Based on these estimations, the expected maximum cladding damage in LFR-600 is fixed as 100 dpa corresponding to the targeted burnup 100 MW d kg^{-1}. The existing results of irradiation testing of FMS (such as 9Cr1Mo, HT9) claddings at temperatures of 670–720 K show that these materials exhibit acceptable swelling and creep rates up to the damage dose of about 200 dpa [25]. Yet, uncertainties still exist on their resistance to the irradiation induced embrittlement and on possible synergy between the corrosion and the irradiation effects, which have not yet been studied.

Specifications of the LFR-600 core with the thermal power of 1500 MW based on the above selected materials and parameters relevant for fuel design are presented in Table 2.

3. Fuel element and core design and configuration

The above developed specifications were used for the preliminary designs of a fuel rod, a fuel assembly and a variant of the LFR-600 core configuration.

3.1. Fuel rod

The next step after the selection of the fuel materials and specifications is the determination of the maximum allowed diameter of a fuel pellet (D_{pel}^{Max}). It can be expressed through the pellet allowed linear heating rate (q_l^{Max}) and the expected maximum power density in fuel (q_v^{Max}):

$$D_{pel}^{Max} = \sqrt{\frac{4 \cdot q_l^{Max}}{\pi \cdot q_v^{Max}}} \quad (1)$$

The expected power density in the fuel of the hottest fuel assembly is determined by the specified fuel maximum burnup (Bu^{Max}), density (ρ_{fuel}) and residence time (t_r):

$$q_v^{Max} = \frac{Bu^{Max} \cdot \rho_{fuel}}{t_r} \quad (2)$$

For the values given in Table 2, Eq. (2) yields $q_v^{Max} \approx 570$ W cm^{-3}.

The allowed linear heating rate depends on the fuel permitted temperature T_{fuel}^{Max} for the normal operation and on the radial thermal resistance $\Re_T$ of a fuel rod (per unit length) between the fuel column centre and the coolant in the peak cross-section (midplane) of the hottest sub-channel. It can be estimated with the following equation:

$$q_l^{Max} = \frac{T_{fuel}^{Max} - T_{cool}^{in} - 0.5 \cdot K_R \cdot \Delta T_{core}}{\Re_T}, \quad (3)$$

where T_{cool}^{in} is the temperature of the Pb-coolant at the core inlet, ΔT_{core} is the coolant temperature increment in the core, K_R – the

Table 2
Tentative specifications for the first ELSY-600 core.

Core parameter	Unit	Value
Electric power	MW	600
Thermal power	MW	1500
Core diameter*	m	⩽6.0
Core active height	m	1.2
Fuel composition	–	$(Pu_yU_{1-y})O_{1.97}$, y = 0.14–0.20
Fuel material density (ρ_{fuel})	kg m^{-3}	~10.5
Fuel discharge HM burnup (Bu^{Max})	MW d kg^{-1}	~100
Fuel residence time (t_r)	a	⩾5
Cladding material	–	Steel T91
Allowable cladding dpa damage	–	100
Allowable cladding normal temperature	K	823
Coolant inlet pressure	MPa	0.6
Coolant inlet temperature (T^{in}_{cool})	K	673
Coolant outlet temperature (T^{out}_{cool})	K	753
Coolant mass flow rate	kg s^{-1}	12 840
Coolant maximum bulk velocity	m s^{-1}	⩽2.0

* The outer diameter of the core barrel.

radial power form-factor of the core ($K_R \leqslant 1.2$ is targeted in the pre-design of the LFR-600 core).

The permitted fuel temperature can be estimated making the assumption that at the end of the fuel residence time it should not exceed the melting temperature in the case of an accidental power excursion or loss of flow accident. A 25% power increase was assumed using the fuel temperature limits recommended for LMFBRs as a landmark.

The melting/solidification temperature of (Pu, U)O_{2-x} fuel (liquidus and solidus) depends on the content of Pu, on the oxygen stoichiometry and on the burnup. The dependence on the stoichiometry is not yet well determined. Some contradictory results were communicated in Ref. [26]. Therefore this dependence is neglected in the following preliminary estimations. The same source [26] reported the liquidus temperature of 3090 ± 50 K and the solidus temperature of 3052 ± 35 K for $Pu_{0.2}U_{0.8}O_{2.00}$, which are in good agreement with the correlations presented in [27], whose authors recommend a liner decrease of the MOX melting temperature with burnup with the rate of 0.5 K per 1 MW d kg^{-1}. This recommendation yields the melting temperature of 3040 K for the MOX with burnup Bu^{Max} = 100 MW d kg^{-1}. Applying some conservatism, it was estimated that the fuel temperature should not exceed 2520 K during the normal operation.

The radial thermal resistance of a fuel rod is a sum of the radial thermal resistances of the pellet, the gap, the cladding and the thermal boundary layer of the Pb-coolant flow:

$$\Re_T = \frac{1}{\pi}\cdot\left(\frac{1}{D_{clad}\cdot h_{cool}} + \frac{\delta_{clad}}{(D_{clad}-\delta_{clad})\cdot\langle\kappa_{clad}\rangle} + \frac{1}{\langle D_{gap}\rangle\cdot h_{gap}} + \frac{1}{4\cdot\langle\kappa_{pel}\rangle}\right) \quad (4)$$

where D_{clad} and $\langle D_{gap}\rangle$ are the clad outer diameter and the gap mean diameter, δ_{clad} – the clad thickness, h_{cool} and h_{gap} are the heat transfer coefficients to the coolant and through the gap, $\langle\kappa_{clad}\rangle$ and $\langle\kappa_{pel}\rangle$ – the mean thermal conductivities of the cladding and the fuel pellet, respectively.

A large uncertainty exists in the correlations recommended for the coefficient of heat transfer (h_{cool}) from the clad to heavy liquid metal flow. The correlation recommended in Ref. [28] was taken for calculations performed in this work. The thermal conductivity of T91 steel was extracted from [29]. It was assumed that pellet–clad gap is just closed by the end of the fuel residence period ($D_{gap} = D_{pel}$), and that a soft contact between the peak pellet and the clad is established. For this situation $h_{gap} \approx 6000$ W m^{-2} K^{-1} was recommended in [30] for preliminary estimations. The MOX thermal conductivity is a function of porosity, stoichiometry, temperature and burnup. Its degradation at high burnups is not well defined yet. The recommendations issued in review [27] are used in these preliminary calculations.

On the basis of the parametric calculations performed with Eqs. (1), (3) and (4), the maximum allowed pellet diameter of 9.1 mm was fixed. A central hole with a diameter of 1.5 mm was also adopted optionally, in order to reduce the maximum temperature, swelling and to smooth the anticipated PCMI. Following the LMFBR [19] and EFR [21,23] analogy and taking into account that approximate mean rate of the irradiation induced swelling of oxide fuel of theoretical density is about 1.6 vol.% per 10 MW d kg^{-1} of HM in a typical fast reactor [31], the radial gap of 0.150 mm and the cladding thickness of 0.6 mm were fixed as the first guess. The allowable equivalent stress of the cladding material (σ^{Max}) was estimated with the following criterion:

$$\sigma^{Max} = \min\left(\frac{\sigma_{uts}}{3.0}, \frac{\sigma_y}{1.5}\right), \quad (5)$$

where σ_{uts} is the ultimate tensile strength and σ_y is the standard yield strength. At the maximum cladding normal temperature of 823 K (see Table 2) Eq. (5) provides $\sigma^{max} \approx 128$ MPa with σ_{uts} and σ_y recommended in [29]. Assuming that main contribution to the clad stress is given by the circumferential stress, the maximum allowable internal pressure for the cladding long-term operation can be estimated as follows [32]:

$$p^{Max}_{plen} = \frac{\sigma^{Max}\cdot\delta_{clad}}{0.5D_{clad} - 0.4\delta_{clad}} \quad (6)$$

At first glance the obtained value of p^{Max}_{plen} = 15 MPa seems to be sufficient to withstand the anticipated release of fission gas from the fuel column and PCMI at the end of the fuel life. The cladding thermal creep is practically negligible at these conditions [29].

The preliminary neutronic estimation of the LFR-600 core sizes, that took into account the limit of 6 m imposed on the core barrel diameter by the mechanical design [11] and the needed reactivity margin, showed that the active fuel height of 1200 mm could be adopted for the pre-design step. Then the total length of the needed gas plenum, estimated based on the experience of LMFBRs, was fixed to be equal to the fuel column length. The preliminary estimations, based on the fission gas yield of 1.17×10^{-3} mol kg^{-1} per 1 MW d kg^{-1} burnup, recommended for MOX in the reference book [20], and the ideal gas equation show that this plenum volume is sufficient for the fuel rod to withstand with a large margin a pressure buildup in the case of the total release of the fission gas from the fuel column at burnup of 100 MW d kg^{-1}. The gas plenum volume is subdivided into two parts: 80% in the lower cold part and 20% in the upper part with a spring. The plenum is filled in with natural helium (He) with pressure p_{He} = 0.2 MPa at T = 300 K. The plenum sizes will be optimized at the next step of the core design. The 10 mm height axial insulation-reflector segments made of yttria stabilized zirconia (YSZ: 94.9 wt% ZrO_2 + 5.1 wt% Y_2O_3) with a density of 6 g cm^{-3} are accommodated between the fuel column and the gas plenum chambers, as shown in Fig. 1(a). The total fuel rod length with top and bottom plugs is 2500 mm.

3.2. Fuel assembly

As it was mentioned in introduction, a hexagonal type fuel assembly has been chosen here for analysis of the LFR-600 fuel performance. The first estimation of the fuel rod pitch in the hexagonal bundle (defined as the 'centre-to-centre' distance between the neighbour rods) was obtained from the thermal balance of the produced and removed heat in the central sub-channel of a fuel rod bundle. Then it was optimized in order to respect two supplemen-

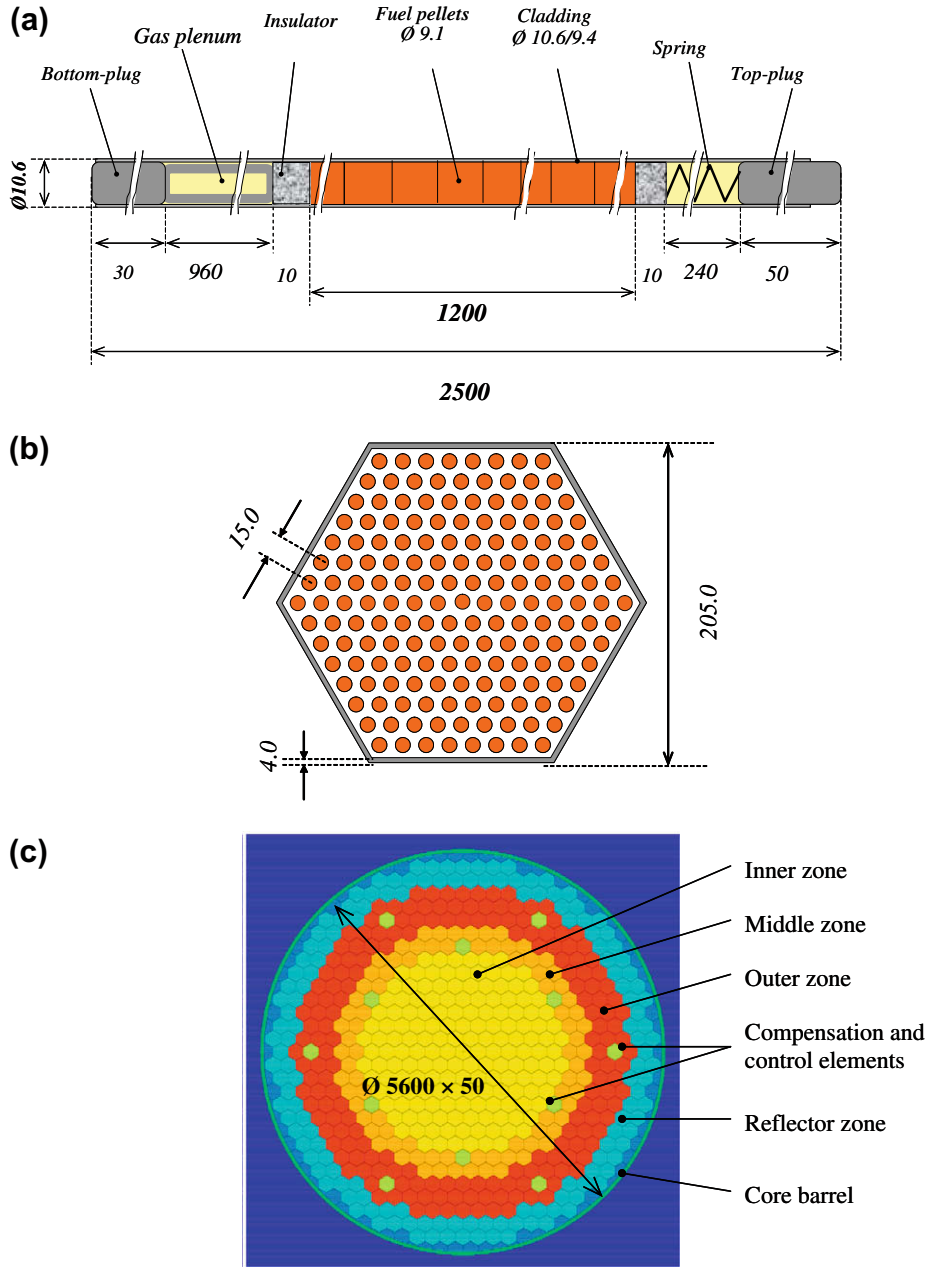

Fig. 1. Axial schematics of a fuel rod (a), radial schematics of a fuel assembly at midplane (b), a variant of the configuration of the three-zone LFR-600 core with the hexagonal fuel assemblies, and (c). Unit: mm.

tary conditions, namely: a coolant bulk velocity $\leqslant 2$ m s^{-1} and a pressure drop $\leqslant 0.1$ MPa on an assembly (the maximum pressure drop of 0.12 MPa between the inlet and outlet plenums of the core was specified in [11]). The correlations recommended in reference books [19,33] for the pressure drop of coolant on a hexagonal bundle of pins was used in calculations. Finally, the rod pitch of 15.0 mm has been fixed. Each hexagonal fuel bundle contains 169 fuel rods. The inner 'plate-to-plate' width of the hexagonal wrapper was estimated as 197 mm. The wrapper is made of T91 steel. Based of the simplified estimations of possible swelling and creep and on the design experience of LMFBRs [19], the wrapper wall thickness of 4.0 mm and a clearance of 5.0 mm between the neighbouring fuel assemblies were adopted. A schematic view of the radial cross-section of the LFR-600 fuel assembly at midplane is presented in Fig. 1(b). The total length of the fuel assembly is 3.8 m. The targeted pressure drop of 0.1 MPa on an assembly is obtained at the Pb-coolant bulk velocity of about 1.6 m s^{-1}.

3.3. Core configuration

After a parametric neutronic analysis of different variants of the LFR-600 core loaded with the fuel elements described above, a reference core configuration shown in Fig. 1(c) has been selected for analysis [24]. This core contains 427 fuel assemblies: 163 in the inner zone, 84 in the intermediate zone and 180 in the outer zone. Twelve positions (six in the intermediate zone and six in the outer zone) are foreseen for absorber elements devoted to the reactivity compensation and control, and for the reactor shutdown. The three-zone active part of the core is surrounded by the radial shielding-reflector zone (144 assemblies with YSZ-pins in the place of MOX-pins) with structure elements and then by the core barrel with the wall thickness of 50 mm and the exterior diameter of 5.6 m.

The enrichment of the various zones is adjusted to flatten the radial power distribution and to obtain a reactivity reserve and a

reactivity loss rate needed for insuring the targeted cycle duration without core reloading.

4. Results of modeling

4.1. Neutronic performances at start

The neutronic modeling of the above designed LFR-600 core was performed with the MCNP5 [34] and ALEPH [35] codes using nuclear data from the JEFF 3.1 library [36]. A critical core at start was considered at the first stage. Preliminary multivariant calculations performed with MCNP5 allowed to fix the fuel enrichment in the different zones as follows: 14.9 at.% Pu in HM in the inner zone, 15.5 at.% Pu in HM in the intermediate zone and 17.4 at.% Pu in the outer zone. This core configuration has the radial power form-factor (the hottest assembly power to the 'mean-assembly' power) of $K_R = 1.10$ and the reactivity reserve of about 1100 pcm (fresh fuel). The calculated 'assembly-by-assembly' power distribution (the ratio of the given assembly power to the core 'mean-assembly' power) is presented in Fig. 2(a) as a function of the radial distance from the core centreline. The axial power in the central assembly is presented in Fig. 2(b); the axial power form-factor is about 1.2. The total power of the hottest assembly is 3.88 MW in the inner zone, 3.91 MW in the middle zone and 3.93 MW in the outer zone. The hottest rod has a total power of 23.25 kW with the peak linear heating rate of 232.5 W cm^{-1}. The main power parameters of the core are given in Table 3. The burnup calculations were performed with the ALEPH code system. It was found that after 1 year of full power operation, the cumulated damage induced by the neutron radiation peaks to 14.5 dpa in the steel cladding of the hottest fuel pin and to 0.07 dpa in the core barrel. The mean rate of the core reactivity loss is of about 200 pcm per year. This indicates that the core can operate, in principle, more than 5 years without reloading.

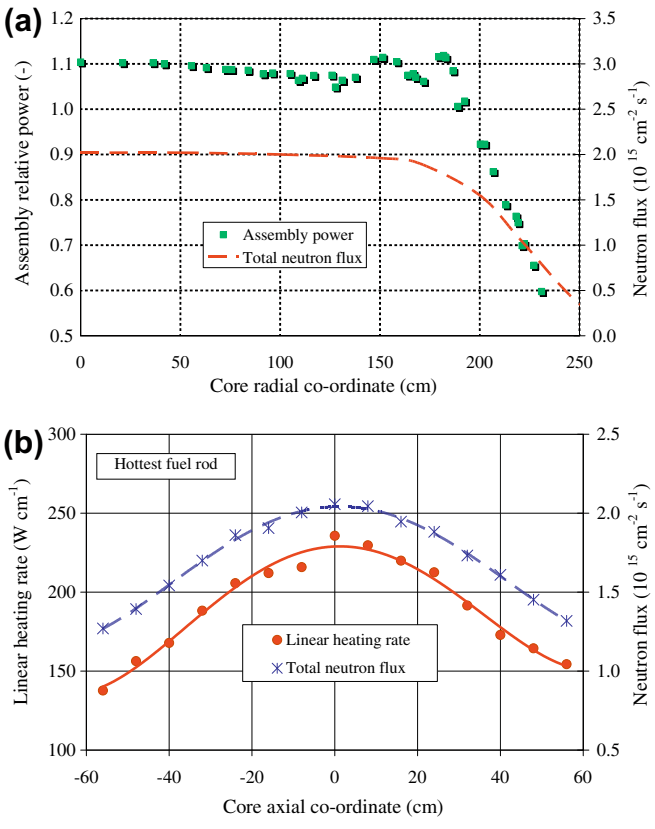

Fig. 2. Radial (a) and axial (b) distributions of power in the LFR-600 core.

Table 3
Main parameters of the proposed variant of the LFR-600 core at BOL.

Core parameter	Unit	Value
Number of active zones	–	3
Number of fuel assemblies	–	427
Number of fuel rods in assembly	–	169
Reserve of reactivity	–	0.0114
Core thermal power	MW	1500
Core average power density within fuel (q_v)	W cm^{-3}	273.5
Core power radial form-factor (K_R)	–	1.10
Core power axial form-factor	–	1.20
Hottest assembly power	MW	3.93
Hottest fuel rod power	kW	23.25
Peak pellet linear power (q_l^{Max})	W cm^{-1}	232.5
Mean rate of reactivity loss	d^{-1}	5.5×10^{-6}
Maximum dpa damage rate in cladding	d^{-1}	0.04
Maximum dpa damage rate in core barrel	d^{-1}	5.5×10^{-5}

4.2. Thermo-mechanical behaviour of the hottest rod

The calculated power distribution in the fuel of the LFR-600 was used for modeling of the thermo-mechanical performances of the hottest fuel rod. For these calculations the fuel performance code FEMAXI-SCK-1 was used, which is under development and testing at SCK•CEN for the pre-design modeling of the mixed oxide fuel behaviour in the fast spectrum systems cooled by liquid lead and lead–bismuth eutectic. For the development of this code, the JAERI codes FEMAXI-V.1 [37], FEMAXI-6 [38] and the burnup module adapted to the fast neutron spectrum were used. The properties database was extended to the Pb–Bi and Pb-coolants [39], to FMS claddings [25,29] and to MOX fuel [27] taking into account supplementary recommendations developed in the FP6 IP EUROTRANS and ELSY [11]. The classical parabolic law was used for growth of the oxidation layer on the cladding outer surface due to oxygen ($\sim 10^{-6}$ wt%) dissolved in the coolant. The corrosion rate was normalized to a value of 25 μm after 1 year of exposure in Pb-flow at $T = 773$ K (500 °C). This value was used as a conservative estimation for the effect of protective layers deposited on T91 steel cladding [18,40]. The corrosion model for the cladding inner surface is still under development and not incorporated yet.

The calculated axial temperature distribution in the elements of the hottest sub-channel of the LFR-600 in 24 h after the reactor start at the nominal power is presented in Fig. 3. The fuel maximum temperature is about 1680 K, which is significantly lower than the permitted temperature limit determined in Section 3 (Fig. 3(a)). The coolant temperature increase in the hottest sub-channel is ~90 K at the Pb bulk velocity of 1.6 m s^{-1} in the active region. At the beginning of the reactor operation, the maximum cladding temperature is 780 K on the outer surface and 790 K on the inner surface (Fig. 3(b)). Both coolant velocity and cladding temperature are also below the specified limits presented in Table 2. After the start, the radial pellet–cladding gap reduces from the designed value of 150 microns ($T = 300$ K) to about 65 microns in the region of the peak pellet due to the pellet cracking, relocation and thermal expansion.

The long-term behaviour of the hottest fuel rod at the nominal conditions was simulated for a period of 2190 effective full power days (EFPD) (this period is equivalent to 6 years of continuous operation at nominal power). The total operation period was subdivided into six one-year cycles with one-month (30 days) shutdown periods in between for maintenance (Fig. 4). The peak fuel burnup of about 80 MW d kg^{-1} and the peak clad damage of 82 dpa are achieved in the end of the operation.

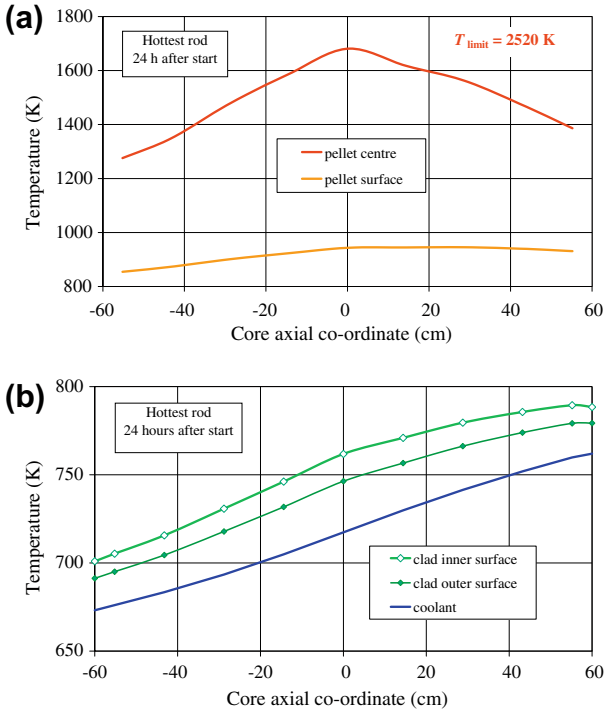

Fig. 3. Axial distribution of temperature in the fuel column (a) and in the cladding (b) of the hottest fuel rod at start.

Figs. 5–7 illustrate the evolution of the fuel and cladding temperatures, of the radial pellet–cladding gap, the contact pellet–cladding stress, the fraction of the released fission gas and the pressure in the gas plenum with time.

The evolution of the central and surface temperatures of the peak pellet and the inside and outside surface temperatures of the cladding are presented in Fig. 5(a) and (b), respectively. From Fig. 5(a) one can see that the peak pellet temperature remains significantly below the fuel permitted temperature in all six operation cycles, indicating that an extension of the operation period is possible. The maximum fuel temperature decreases in the first cycle, due to the irradiation induced fuel re-sintering (densification). After completion of the densification, it begins to increase. Two factors affect this increase: the irradiation induced degradation of the fuel thermal conductivity and a variation of the thermal conductance of the pellet–cladding gap induced by the fission gas release from the fuel into the gap (Fig. 6) and by the gap thickness reduction (Fig. 7). The fuel thermal conductivity decreases permanently

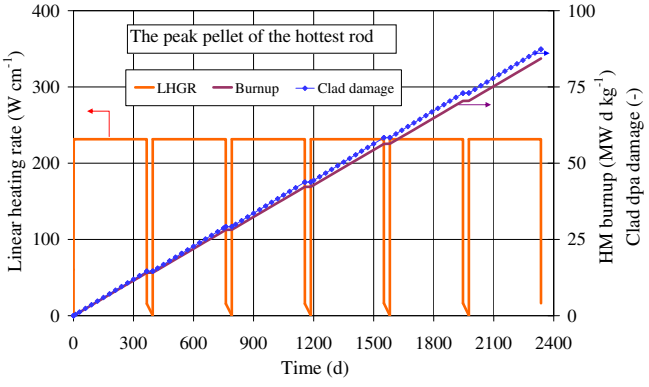

Fig. 4. Operation history (linear heating rate) of the hottest fuel rod.

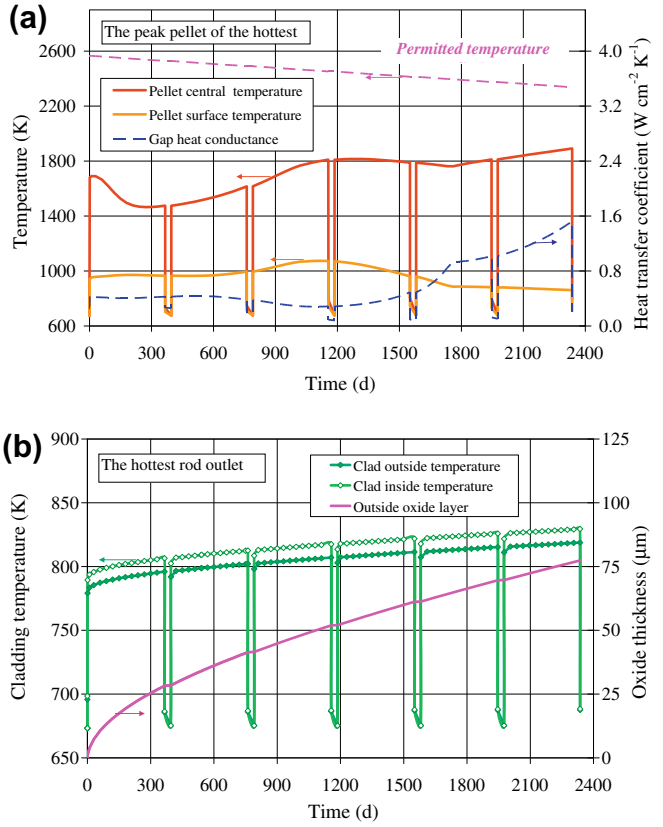

Fig. 5. Evolution of the central and surface temperatures of the peak fuel pellet (a) and of the cladding (b) in the hottest fuel rod.

with irradiation, resulting in the growth of the radial temperature difference across the fuel pellets (Fig. 5(a)). The variation of the gap conductance leads to the variation of the pellet surface temperature. A week decrease of the gap thermal conductance during the third cycle is attributed to the contamination of the initial filling gas (He) by the fission gas (Xe and Kr) released from the fuel column (Fig. 6). Its rapid increase in the fourth, fifth and sixth cycles is due to the gap closing followed by the increase in the contact pressure between the pellet and the cladding (Fig. 7).

Fig. 5(b) illustrates the effect of corrosion on the cladding outer temperature. The cladding outer temperature increases from 780 K at start up to 820 K by the end of operation with the growth of the corrosion layer. This still satisfies the initial specifications (Table 2). It should be noted, however, that these results are very sensitive to the corrosion protection technology (a higher corrosion rate would be obtained in the case of utilization of the well-known oxygen protection technology without special protective layer [12]).

Intensive release of fission gas in the hottest fuel rod starts in the middle of the second cycle, and its rate increases during the third cycle. Then it is stabilized at the level of about 40% of the fission gas production (Fig. 6). The gas plenum pressure continuously increases with the gas release and reaches about of 2.6 MPa by the end of operation. This pressure is few times lower then the designed limit.

The evolution of the pellet–cladding gap thickness is illustrated in Fig. 7. After the pellet cracking and relocation at start, it increases in the beginning of the first cycle due to the fuel densification. Since the middle of the first cycle (when the fuel densification is completed), the gap decreases due to the irradiation induced fuel swelling until the complete closing in the middle of the fifth cycle. Then the peak pellet enters in contact with the cladding, and a

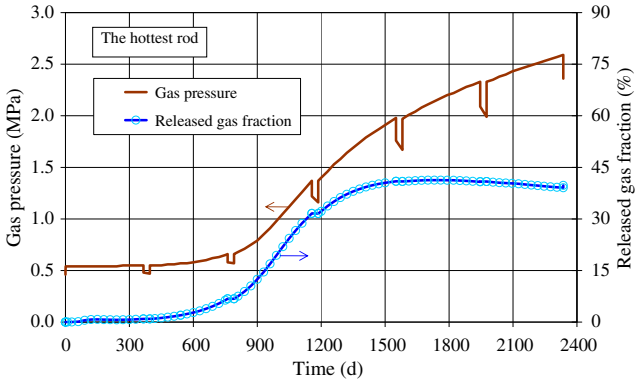

Fig. 6. Evolution of fission gas release and pressure in the hottest rod.

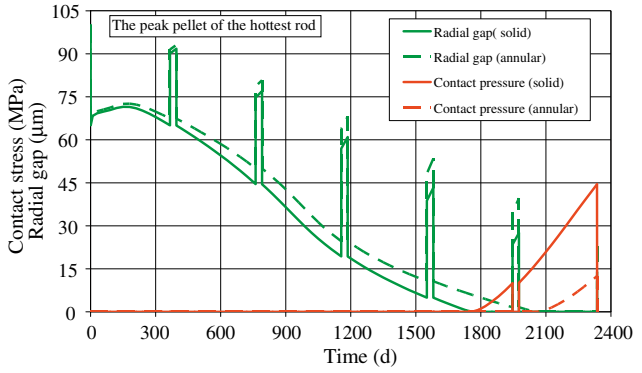

Fig. 7. Evolution of the radial pellet–cladding gap and the pellet–cladding contact stress in the hottest fuel rod.

supplementary contact stress is built in the cladding. The contact stress magnitude increases with irradiation time: it is about 10 MPa in the end of the fifth cycle, and reaches 45 MPa by the end of operation. This stress is still lower than the limit allowed for the normal operation, but PCMI can be dangerous in the case of temperature transients. Therefore, mitigating actions (such as a periodic core reshuffling or modifications in fuel design) should be envisaged to avoid PCMI. One of the possible solutions is to replace solid pellets by annular pellets. It will allow reducing the fuel temperature and will provide more free space for the swelling [41]. This variant was analysed as an alternative option in the design proposal. The effect of annular pellets with the central hole of 1.5 mm on PCMI in the hottest rod is shown in Fig. 7. It can be seen that in this case the pellet–cladding gap remains open until the beginning of the sixth cycle, and the contact stress drops from 45 to about 14 MPa in the end of operation.

5. Conclusions

Based on the specifications of the GEN-IV ELSY and the neutronic and thermal parametric studies, the preliminary designs of the fuel rod, the hexagonal fuel assembly and the core configuration have been developed for the LFR-600 system. The proposed configuration of the core with thermal power of 1500 MW is composed of 427 MOX fuel assemblies with the active height of 1.2 m arranged in three zones with different Pu-enrichments: 163 assemblies with 14.9 at.% Pu MOX in the inner zone, 84 assemblies with 15.5 at.% Pu MOX in the middle and 180 assemblies with 17.4 at.% Pu MOX in the outer. The maximum radial power form-factor of about 1.10 and the maximum axial power form-factor of 1.20 at the beginning of the core life were obtained. A reactivity excess of 1100 pcm can permit more that 5 years operation without refueling.

The results of simulation of the long-term thermo-mechanical behaviour of the hottest fuel rod show that it can withstand the normal operation conditions of the LFR-600 during about six years. The fuel maximum burnup of ~80 MW d kg^{-1} and the clad maximum damage of about 82 dpa are achieved in the end of this period. PCMI can arise in the fifth and sixth cycles, which is partially compensated by the clad creep. Annular fuel pellets can improve the situation. Further optimization of the LFR-600 core and fuel design is needed in order to avoid PCMI and to achieve the targeted burnup of 100 MW d kg^{-1}.

Acknowledgements

This work was supported by funds of the EURATOM FP6 ELSY Project and of the MYRRHA Project of the Belgian Nuclear Research Centre SCK•CEN.

References

[1] A technology roadmap for Generation IV nuclear energy systems. GIF-002-00, USDOE Nuclear Energy Research Advisory Committee and the Generation IV International Forum, December 2002.
[2] V.V. Orlov, V.N. Leonov, A.G. Sila-Novitskij, V.S. Smirnov, A.I. Filin, V.S. Tsikunov, in: Proceedings of the International Conference on Heavy Liquid Metal Coolants in Nuclear Technology - HLMC'98, vol. 2, Obninsk, Russian Federation, 5–9 October 1998, Obninsk: SSC RF - IPPE, 1999, p. 462.
[3] A.V. Zrodnikov, G.I. Toshinskii, O.G. Grigor'ev, Yu.G. Dragunov, V.S. Stepanov, N.N. Klimov, I.I. Kopytov, V.N. Krushel'nitskii, A.A. Grudakov, Atomic Energy 97 (2004) 528.
[4] M. Takahashi, S. Uchida, Bulletin – Research Laboratory for Nuclear Reactors 30 (2006) 206.
[5] T. Nakazima, A.K. Rivai, K. Hata, V. Dostal, M. Takahashi, in: Proceedings of the Fourteenth International Conference on Nuclear Engineering – ICONE 14, Miami – Florida, USA, 17–20 July 2006, Paper 89420.
[6] H. Sekimoto, K. Ryu, Y. Yoshimura, Nucl. Sci. Eng. 139 (2001) 306.
[7] J.-Y. Lim, M.-H. Kim, Progr. Nucl. Energy 49 (2007) 230.
[8] Y.H. Yu, H.M. Son, I.S. Lee, K.Y. Suh, in: Proceedings of the International Conference on Advances in Nuclear Power Plants - ICAPP'06, Reno – Nevada, USA, 4–8 June 2006, Paper 6148.
[9] J.J. Sienicki, A.V. Moisseytsev, in: Proceedings of the International Conference on Advances in Nuclear Power Plants - ICAPP'05, Seoul, Korea, 15–19 May 2005, Paper 5426.
[10] L. Cinotti, C.F. Smith, J.J. Sienicki, H. Aït Abderrahim, G. Benamati, G. Locatelli, S. Monti, H. Wider, D. Struwe, A. Orden, in: Proceedings of the International Congress on Advances in Nuclear Power Plants – ICAPP'07, Nice, France, May 13–18 2007, Paper 7585.
[11] L. Cinotti, H. Aït Abderrahim, G. Benamati, C. Fazio, J. Knebel, G. Locatelli, S. Monti, C.F. Smith, K. Suh, in: Proceedings of the Conference on EU Research and Training in Reactor Systems – FISA 2006, Luxembourg, 13–16 March 2006, Document EUR 21231, FISA 2006, European Commission, Luxembourg, 2006, p. 248.
[12] G.S. Yachmenyov, A.Ye. Rusanov, B.F. Gromov, Yu. S. Belomytsev, N.S. Skvortsov, A.P. Demishonkov, in: Proceedings of the International Conference on Heavy Liquid Metal Coolants in Nuclear Technology - HLMC'98, vol. 1, Obninsk, Russian Federation, 5–9 October 1998, Obninsk: SSC RF - IPPE, 1999, p. 133.
[13] R.L. Klueh, A.T. Nelson, J. Nucl. Mater. 371 (2007) 37.
[14] R.L. Klueh, D.S. Gelles, S. Jitsukawa, A. Kimura, G.R. Odette, B. van der Schaaf, M. Victoria, J. Nucl. Mater. 307–311 (2002) 455.
[15] D.P. Park, C.A. Butt Beard, Nucl. Eng. Design 196 (3) (2000) 315.
[16] B.F. Gromov, Y.I. Orlov, P.N. Martynov, V.A. Gulevsky, in: Proceedings of the International Conference on Heavy Liquid Metal Coolants in Nuclear Technology - HLMC'98, vol. 1, Obninsk, Russian Federation, 5–9 October 1998, Obninsk: SSC RF - IPPE, 1999, p. 120.
[17] G. Müller, A. Heinzel, J. Konys, G. Schmacher, A. Weisenburger, F. Zimmermann, V. Engelgo, A. Rusanov, V. Markov, J. Nucl. Mater. 301 (2002) 40.
[18] A. Weisenburger, A. Heinzel, G. Müller, H. Muscher, A. Rousanov, J. Nucl. Mater. 376 (2008) 274.
[19] A.E. Waltar, A.B. Reynolds, Fast Breeder Reactors, Pergamon, New York, 1980.
[20] H. Bailly, D. Ménissier, C. Prunier, Le Combustible Nucléaire des Réacteurs à Eau Sous Pression et des Réacteurs à Neutrons Rapides, CEA, Eyrolles, Paris, 1996.
[21] M. Köhler, H. Noel, A. Green, in: Proceedings of the International Fast Reactor Safety Meeting, Snowbird, Utah, USA, 12–16 August 1990.
[22] J.C. Lefevre, C.H. Mitchell, G. Hubert, Nucl. Eng. Design 162 (1996) 133.
[23] M. Asty, in: Proceedings of the 27 Meeting of International Working Group on Fast Reactors, Vienna, Austria, 17–19 May 1994, IAEA TECDOC-791, p. 88.

[24] E. Malambu, V. Sobolev, N. Messaoudi, H. Aït Abderrahim, D. Struwe, M. Schikorr, E. Bubelis, in: Proceedings of the International Conference on the Physics of Reactors Nuclear Power: A Sustainable Resource - PHYSOR-2008, Interlaken, Switzerland, 14–19 September 2008, Paper FP 493 (in press).
[25] M.B. Toloczko, F.A. Garner, C.R. Eiholzer, J. Nucl. Mater. 212–215 (1994) 604.
[26] M. Kato, K. Morimoto, H. Sugata, K. Konashi, M. Kashimura, T. Abe, J. Alloys Comp. 452 (2008) 48.
[27] J.J. Carbajo, G.L. Yoder, S.G. Popov, V.K. Ivanov, J. Nucl. Mater. 299 (2001) 181.
[28] A.V. Zhukov, Yu.A. Kuzina, A.P. Sorokin, V.N. Leonov, V.P. Smirnov, A.G. Sila-Novitskii, Thermal Eng. 49 (3) (2002) 175.
[29] K. Haarmann, J.C. Vaillant, W. Bendick, A. Arbab, The T91/P91 Book, Vallourec & Mannesmann Tubes, Houston, USA, 1999.
[30] S. Glasstone, A. Sesonske, Nuclear Reactor Engineering, Van Nostrand Reinold Company, New York, 1980.
[31] K. Wirtz, Lectures on Fast Reactors, Kernforschungszentrum und Universität Karlsruhe, Karlsruhe, Germany, 1978.
[32] ASME Boiler & Pressure Vessel Code, Section VIII, Division 1, Subsection A, Article UG-27, ASME, New York, 1998.
[33] I.E. Idel'chic, Mémento des Pertes de Charge, Eyrolles, Paris, 1986.
[34] X-5 Monte-Carlo Team: MCNP – A General Monte-Carlo N-Particle Transport Code, Version 5, LANL, Los Alamos, New Mexico, USA, April 2003.
[35] W. Haeck, B. Verboomen, Nucl. Sci. Eng. 156 (2007) 180.
[36] W. Haeck, B. Verboomen, Validated MCNP(X) Cross-Section Library based on JEFF 3.1, SCK•CEN Report BLG-1034, Mol, Belgium, October 2006 (see also <http://www.nea.fr/abs/html/nea-1745.html>).
[37] M. Suzuki, Light Water Reactor Fuel Analysis Code FEMAXI-V, JAERI Report, Tokai-Mura, Japan, January 2001.
[38] M. Suzuki, H. Saitou, Light Water Reactor Fuel Analysis Code FEMAXI-6 (Ver.1), JAEA-Data/Code 2005–003, Tokai-Mura, Japan, 2006 (see also <http://www.nea.fr/abs/html/nea-1080.html>).
[39] V. Sobolev, J. Nucl. Mater. 362 (2007) 235.
[40] G. Müller, A. Heinzel, J. Konys, G. Schumacher, A. Weisenburger, F. Zimmermann, V. Engelko, A. Rusanov, V. Markov, J. Nucl. Mater. 335 (2004) 163.
[41] D.R. Olander, Fundamental Aspects of Nuclear Reactor Fuel Elements, ERDA Technical Information Service, Oak-Ridge, Tennessee, USA, 1976.